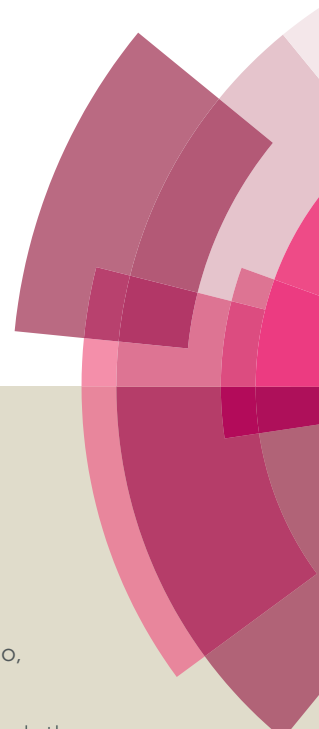


# Catalysis Science & Technology

Accepted Manuscript



This article can be cited before page numbers have been issued, to do this please use: H. Zhang, J. Gao, Z. Zhao, G. Z. Chen, T. Wu and F. He, *Catal. Sci. Technol.*, 2016, DOI: 10.1039/C5CY02133B.



This is an *Accepted Manuscript*, which has been through the Royal Society of Chemistry peer review process and has been accepted for publication.

*Accepted Manuscripts* are published online shortly after acceptance, before technical editing, formatting and proof reading. Using this free service, authors can make their results available to the community, in citable form, before we publish the edited article. We will replace this *Accepted Manuscript* with the edited and formatted *Advance Article* as soon as it is available.

You can find more information about *Accepted Manuscripts* in the [Information for Authors](#).

Please note that technical editing may introduce minor changes to the text and/or graphics, which may alter content. The journal's standard [Terms & Conditions](#) and the [Ethical guidelines](#) still apply. In no event shall the Royal Society of Chemistry be held responsible for any errors or omissions in this *Accepted Manuscript* or any consequences arising from the use of any information it contains.



## Catalysis Science &amp; Technology

## ARTICLE

## Esterification of Fatty Acids from Waste Cooking Oil to Biodiesel Over a Sulfonated Resin/PVA Composite

Honglei Zhang,<sup>a,b</sup> Jiarui Gao,<sup>a</sup> Zengdian Zhao,<sup>c</sup> George Z. Chen,<sup>a,b,d</sup> Tao Wu,<sup>a</sup> and Feng He<sup>e\*</sup>

Received 00th January 20xx,  
Accepted 00th January 20xx

DOI: 10.1039/x0xx00000x  
[www.rsc.org/](http://www.rsc.org/)

Sulfonated cation exchange resins (s-CER) have been widely studied as a replacement of liquid acids for the catalysis of esterification of free fatty acids (FFAs) to produce biodiesel with water as the only by-product. However, the water produced has strong affinity to sulfonate groups in s-CER, which blocks the reactive sites for esterification and thus reduces the activity of the catalyst. To overcome this technical barrier, we have designed an s-CER/PVA composite by incorporating s-CER fines within a poly (vinyl alcohol) (PVA) matrix. PVA has much stronger absorption preference of water than s-CER and has very low selectivity for the reactants (FFAs and methanol), which enables the continuous removal of the produced water and liberation of reactive sulfonate sites in s-CER for catalysis. With s-CER/PVA, the FFAs conversion was increased from 80.1% to 97.5% after 8-hour reaction and the turnover frequency (TOF) was increased more than 3.3 times. The TOF of s-CER/PVA was also 2.6 times of that of sulfuric acid, suggesting that the water less, heterogeneous sulfonate sites are more reactive than water-blocked homogeneous ones. The reusability of the s-CER/PVA was also enhanced due to that the produced water that could cause deactivation of the s-CER was largely removed by PVA.

### 1. Introduction

Biodiesel is a non-petroleum-based fuel that consists of alkyl esters derived from either the transesterification of triglycerides or the esterification of free fatty acids (FFAs) with low molecular weight alcohols.<sup>1</sup> Made from renewable resources such as plant oils and animal fats, biodiesel is biodegradable, renewable, less toxic and easier to store.<sup>2, 3</sup> It can be used in current engines directly or blended with petroleum-based diesel fuels. However, biodiesel has not currently become competitive compared with fossil fuels due to its higher cost of raw material and production.<sup>4, 5</sup> One way to reduce the cost of biodiesel is to use a cheaper oil feed like waste cooking oil (WCO).<sup>6</sup> However, WCO requires pretreatment for biodiesel production because of its high FFAs content, which produces soap during base-catalyzed transesterification.<sup>7</sup> Therefore, esterification of FFAs in WCO is often catalyzed by homogeneous strong acids, such as sulfuric acid first and followed by transesterification.<sup>8</sup> However, the use of liquid acids for esterification causes many

problems, such as difficulty of biodiesel separation from reaction medium, formation of large amount of wastewater and significant corrosion of equipment.<sup>9-11</sup>

Sulfonated (or strong acid) cation exchange resins (s-CER), composed of copolymers of divinyl-benzene, styrene with sulfonate (-SO<sub>3</sub>H) groups grafted on the benzene rings, have been proposed to replace liquid acids for esterification because they are non-corrosive and easy to be separated from reaction mixture.<sup>12-15</sup> Also s-CER can offer better selectivity towards the desired product(s) and better reusability compared with homogeneous acid catalysts.<sup>14</sup> However, due to their particular cross-linked structure, s-CER are subjected to remarkable swelling when contacted with polar solvents like water.<sup>16, 17</sup> One -SO<sub>3</sub>H groups in s-CER can collect about 8-12 water molecules and the absorbed water can cover the internal surface of resin and block the reactive sulfonate sites, thus reducing the catalytic activity.<sup>18</sup> Therefore, to enhance the efficiency of esterification catalyzed by s-CER, it is essential to reduce the absorption of water to sulfonate groups. However, until now there are almost no efforts on modification of s-CER to achieve this goal.

Poly (vinyl alcohol) (PVA), a water-absorbing polymer, is commonly used as a polymeric material to prepare membrane since it displays good mechanical strength, high thermal stability and good chemical resistance.<sup>19-24</sup> Because of its superior hydrophilicity, citric acid (CA) cross-linked PVA membrane has been used as a pervaporation membrane to separate water during esterification but not as a catalyst support.<sup>22</sup> In addition, PVA was used as a main membrane matrix to prepare poly (styrene sulfonic acid) (PSSA)/PVA membrane for catalyzing esterification although its role as a water absorber was not recognized.<sup>19</sup> Based on these results, we hypothesize that incorporating commercial s-CER in the matrix of PVA can provide a way to continuously remove the produced water from sulfonate sites of s-CER to PVA during esterification and therefore not only enhance the catalytic activity of s-CER but also reduce water separation steps in biodiesel production.

<sup>a</sup>Key Laboratory of Clean Energy Conversion Technologies, The University of Nottingham Ningbo China, P.R. China

<sup>b</sup> Department of Chemical and Environmental Engineering, Faculty of Engineering, The University of Nottingham, Nottingham, NG7 2RD, UK

<sup>c</sup> School of Chemical Engineering, Shandong University of Technology, Zibo, 255049, P. R. China,

<sup>d</sup> International Academy of Marine Economy and Technology, The University of Nottingham Ningbo China, Ningbo, 315100, P.R. China

<sup>e</sup> College of Environment, Zhejiang University of Technology, Hangzhou, Zhejiang 310032, China. Email: fenghe@zjut.edu.cn; 086-571-88320054 (ph); 086-571-88320054(fax).

Electronic Supplementary Information (ESI) available: [details of any supplementary information available should be included here]. See DOI: 10.1039/c000000x/

In this work, an s-CER/PVA composite was prepared by entrapping fractured s-CER particles within a PVA matrix. The s-CER was grounded to fine particles before use to maximally expose catalytic sites for esterification. The s-CER/PVA was employed for the catalysis of esterification of FFAs with methanol for biodiesel production. We show that PVA has a much stronger preference for water than s-CER and has very little affinity for FFAs and methanol. Therefore, PVA only removes product with side effects (i.e., H<sub>2</sub>O) but does not compete for reactants. As a result, s-CER/PVA converted 17.0 % more FFAs to biodiesel after esterification reached steady state and showed 3.3 times higher turnover frequency (TOF) than s-CER alone. We also demonstrate that the structure and consequently the catalytic activity of s-CER/PVA are significantly affected by the s-CER: PVA mass ratio and the annealing temperatures of the composite. In addition, the FFAs conversion only reduced from 97.5 % to 85.0 % after 6 runs without removing any produced water.

## 2. Experimental Section

### 2.1 Materials

The FFAs (average M.W. = 371 g mol<sup>-1</sup>) obtained from waste cooking oil was supplied by Haolin Bioenergy Company (Hubei, China). The main compositions of the FFAs were determined to be dodecanoic acid, tetradecanoic acid, hexadecanoic acid and octadecadienoic acid using a GC-MS (6890N GC/5973 MS, Agilent). PVA with a polymerization degree of 1750±50 was obtained from Tianjin Kermel Chemical Reagents Ltd., China. The s-CER provided by Nankai Group (Tianjin, China) was milled in frozen state using liquid nitrogen to obtain fragments (~24.96 μm) and then used in control experiments and composite synthesis. The detailed information of the s-CER and FFAs is provided in Table S1 and S2 in Electronic Supplementary Information (ESI), respectively.

### 2.2 S-CER/PVA preparation

PVA solutions were prepared at 363 K under continuous stirring for 6 h, and then 8-16 g of the grounded s-CER particles was added into the above solution and stirred at 323 K till a homogeneous solution formed. The solution was cast onto a glass plate and immersed into ethanol/water coagulation bath for phase inversion. A variety of ethanol percentages were used to obtain s-CER/PVA composites with different porosities (Table S3). Then the wet composites were peeled off from the plate and dried at 323 K for 24 h to obtain dry s-CER/PVA flakes. The composite flakes were further annealed at 323, 373 and 423 K in N<sub>2</sub> atmosphere, respectively, for 1 h. The thicknesses of the resulting composite flakes were in the range of 0.20-0.40 mm.

### 2.3 Physical characterization

The s-CER/PVA composite samples were freeze-dried at 213 K in vacuum and then fractured to expose the cross-sectional area in liquid nitrogen. The composite samples for measurement of scanning electron microscope (SEM) were coated by gold via sputtering at 20 mA for 180 s. The cross-section morphology of the composite was inspected under a Zeiss Ultra plus field-emission scanning electron microscope (FESEM) (Zeiss Co.) equipped with an energy dispersive X-ray (EDX) detector operating at an accelerating voltage of 10 kV. The composites annealed at different temperatures were characterized by a TENSOR-37 Fourier transform infrared spectroscopy (FTIR) (Bruker Co.) operated by attenuated total reflectance (ATR) in the wave number range of 4000-500 cm<sup>-1</sup>. The thermal stability of the composites was investigated using a STA449 F3 Jupiter (Netzsch Co.). Thermo gravimetric analysis (TGA)

was carried out under a nitrogen atmosphere at a heating rate of 10 K min<sup>-1</sup> from 323 to 773 K. Ion exchange capacity (IEC) indicates the number of milli equivalents of ions (H<sup>+</sup>) in dry composite of unit quality.<sup>13</sup> The IEC of the composites was obtained using the KOH titration method. The reported values were the mean of at least five measurements and the average experimental error was ±5 %. Swelling degree (SD) represents the swelling status of the composite in the solvent and was measured according to Caetano's method.<sup>25</sup> SD was calculated by dividing the initial sample mass by the mass difference between swollen sample and initial sample. The porosity of the composite flake was obtained by dividing the mass difference between dry and water-saturated composite by area and thickness according to Ding's method.<sup>26</sup> Sulfur content in the FFAs and biodiesel were tested by a micro-coulometry analyzer (WK-2D, Jianfen Electrochemical Instrument CO., LTD. China) and water content was detected by a Karl Fischer water tester. The elemental composition of the samples was studied by elemental analysis with a Perkin-Elmer 2400 Series II CHNS/O analyzer (PerkinElmer Co.). Analyses of FFAs and FAME were performed on a GC (7890B, Agilent) equipped with a HP-5 column. The temperatures of the injector and FID detector were both at 523 K. The oven temperature was ramped from 333 K to 513 K at a rate of 10 K min<sup>-1</sup> and held at 513 K for 10 min.

### 2.4 Esterification catalyzed by s-CER/PVA

Esterification reactions were performed in a three-necked batch reactor (250 mL) equipped with a reflux condenser and a mechanical stirrer at atmospheric pressure. The composite flakes were cut into small pieces (about 0.5 cm × 0.5 cm) to achieve better contact with the reactants and to remove the influence of diffusion on esterification. The reaction temperature was controlled using a heating jacket and a thermocouple. The primary reaction conditions were as following: FFAs 20 g; methanol: FFAs mass ratio 2.5: 1 (equivalent to molar ratio 29: 1); composite loading 4 g; mechanical stirring rate 360 rpm; reaction temperature 338 K; and reaction time 8 h, except otherwise mentioned. The optimal reaction conditions were comprehensively studied (Fig. S1) and the results are listed in Section 3.6. The acid value of oil was determined by KOH titration according to ISO 660: 2009 and used for FFAs conversion calculation. The fatty acid methyl esters (FAME) produced from esterification under optimal reaction conditions were determined using GC-MS (see Table S4). The FAME yield along with FFAs conversion were then quantified using a GC (7890B, Agilent) after calibrated using corresponding FFA and FAME standards. All the esterification reactions were at least triplicated and the reported FFAs conversion was the mean with standard deviation. More details on the esterification experiments are provided in ESI.

For kinetic studies, the conversion results in the first 4 hours were fitted to a pseudo-first order rate equation to determine the rate constant *k*. TOF was defined as the number of molecules of a specified product formed per catalytic active site and per unit time.<sup>27</sup> Here, the initial TOF was calculated according to the equation below,

$$TOF = k \frac{n_0}{n_{H^+}}$$

where, *k* is the first-order reaction rate constant, *n*<sub>0</sub> is the moles of FFAs at *t* = 0, and *n*<sub>H<sup>+</sup></sub> is the moles of equivalent H<sup>+</sup> in the catalyst.

## 3. Results and Discussion

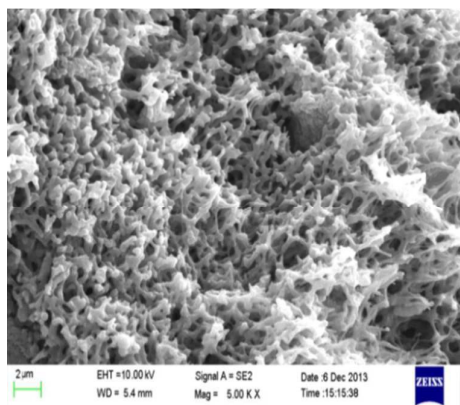


**Fig. 1** SEM image of cross-section obtained from s-CER/PVA annealed at 373 K (at 5000 $\times$ ).

### 3.1 Characterization of the composites

SEM images of the cross section of the s-CER/PVA composite flake annealed at 373 K showed a spongy and porous structure generated by the addition of PVA (Fig. 1). The measured porosities of the s-CER/PVA (mass ratio 3: 2) synthesized using different ethanol/water ratios for phase inversion were 43.7 to 54.3 % (Table S3), which is in agreement with the SEM observations. The existence of fairly uniform pore size and distribution in the polymer matrix is beneficial for the reactants to flow smoothly onto the entrapped resin fines and thus realize the catalytic process.

To understand the effect of annealing, TGA of the PVA, s-CER and s-CER/PVA composite (mass ratio 3: 2) annealed at 323, 373, and 423 K were carried out and the results are illustrated in Fig. 2. TGA curves of PVA involves three main degradation stages due to loss of absorbed water (up to 393 K),<sup>19</sup> dehydroxylation (393-503 K) and decomposition of the PVA main chains (above 540 K).<sup>28, 29</sup> TGA curve of s-CER has two degradation stages at up to 393 K and above 480 K, which are the weight loss of absorbed water and sulfonate groups, respectively. However, TGA curves of s-CER/PVA consist of four main degradation stages arising from the processes of desolvation, dehydroxylation, desulfonation and decomposition of the polymer main chains. The first weight loss up to 393 K was closely associated with the removal of absorbed water in composite matrix. Therefore, the annealing processes at 323 and 373 K only remove absorbed water. At this stage, the weight losses were 12.5, 8.0 and 5.5 wt % for the composite annealed at 323, 373 and 423 K respectively, which indicates that the water content decreased with the increase of annealing temperature. The second weight loss region between 393 and 503 K mainly came from the dehydroxylation of PVA.<sup>19</sup> The weight loss of the composites became much smaller (from 34.0 to 15.0 wt %) as the annealing temperature increased from 323 to 423 K. This indicates that the -OH content in the composite was reduced due to dehydroxylation when annealed at 423 K. The third weight loss region at the temperature of 520-670 K was mainly due to the loss of sulfonate groups in s-CER.<sup>30</sup> The weight losses at this stage were 11.0, 13.0 and 15.0 wt % for composites annealed at 323, 373, and 423 K, respectively. Since these three composites contained the same amount of s-CER and the annealing temperatures were far below 480 K, the increased -SO<sub>3</sub>H content is a result of the loss of water and/or -OH groups at higher annealing temperatures. In the fourth weight loss region at temperature above 670 K, the polymer residues were further degraded due to decomposition of the main chain of PVA.

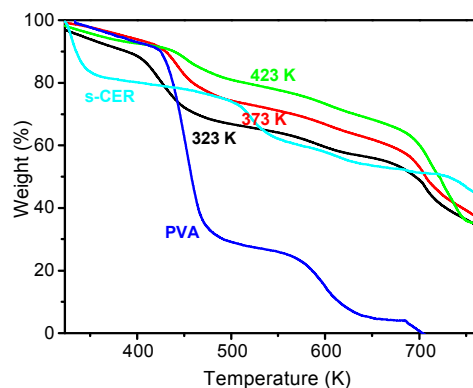


**Fig. 2** TGA curves of PVA, s-CER and s-CER/PVA composites (3:2 mass ratio) annealed at 323, 373 and 423 K.

FTIR spectra of s-CER/PVA (mass ratio 3: 2) annealed at 323, 372, and 423 K are shown in Fig. 3 and Fig. S2. The FTIR curve of PVA exhibits three strong peaks at 1088, 1407 and 3264  $\text{cm}^{-1}$ , which represent the stretching vibration of C-OH, the deformation vibration of O-H and the stretching band of O-H, respectively. The FTIR curve of s-CER has three strong peaks at 1006, 1035 and 1170  $\text{cm}^{-1}$ , which are believed to be symmetric O=S=O stretching vibrations and S-C stretching vibration of -SO<sub>3</sub>H groups.<sup>31, 32</sup> As for the FTIR curves of s-CER/PVA, it can be seen that the peaks at 1088  $\text{cm}^{-1}$  and 1407  $\text{cm}^{-1}$  become weaker with the annealing temperature increased from 323 to 423 K. This strongly suggests that the -OH content in PVA decreased when annealed at 423 K, likely due to dehydroxylation (based on TGA analysis). At the same time, the peak of the O-H stretching band shifts from 3300  $\text{cm}^{-1}$  in the s-CER/PVA composite annealed at 323 K to 3388  $\text{cm}^{-1}$  in the composite annealed at 423 K. This indicates that the -OH groups reacted with other reactive groups in s-CER at 423 K.<sup>19, 33, 34</sup> In addition, the sharp peak at 1035  $\text{cm}^{-1}$  associated with symmetric O=S=O stretching vibrations becomes weaker at 423 K. In addition, there is no peak at 772  $\text{cm}^{-1}$  for the O<sub>2</sub>S-O-C bond of sulfonic acid ester<sup>19, 33</sup> in the pure s-CER sample (Fig. S2 (a)), however, this peak appears in the s-CER: PVA annealed at 323 K and becomes obviously stronger in that annealed at 423 K. This fact suggests that O<sub>2</sub>S-O-C bond was formed during the annealing process. Also, the peaks at 1006 and 1035  $\text{cm}^{-1}$  become weaker with the increase of annealing temperature. The combined information indicates that the -OH groups reacted with the -SO<sub>3</sub>H to form sulfonic acid ester in s-CER/PVA during annealing especially at high temperatures.

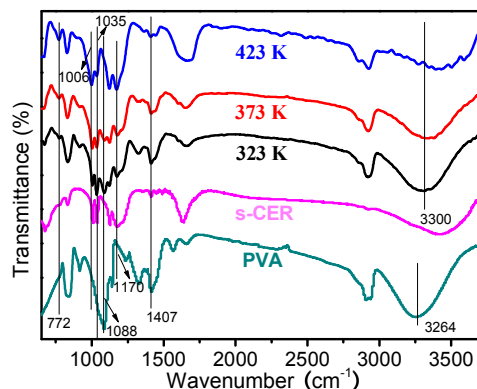


**Fig. 3** FTIR spectra of PVA, s-CER and s-CER/PVA composites (mass ratio 3: 2) annealed at 323, 373 and 423 K.

**Table 1** IEC of s-CER/PVA composite ( $\text{mmol g}^{-1}$ ) with different s-CER: PVA mass ratios.

Annealing temperature	S-CER: PVA mass ratio			
	1: 1	5: 4	3: 2	2: 1
323 K	1.72	1.73	1.87	2.56
373 K	1.90	1.96	2.01	2.75
423 K	1.49	1.57	1.62	2.03

Ion exchange capacity (IEC) of composites with different s-CER: PVA mass ratios annealed at different temperatures are listed in Table 1. The IEC of composite annealed at 373 K was higher than that of composites annealed at 323 K with the same s-CER: PVA mass ratio due to the decreased water content in the composites (based on TGA analysis). IEC decreased with the annealing temperature increased from 373 to 423 K, likely because the sulfonate groups in s-CER reacted with the hydroxyl groups of PVA when annealed at 423 K (based on FTIR results), which decreased the number of sulfonate groups and led to the decrease of IEC. For the composites with different s-CER: PVA mass ratios, IEC increased with the increase of s-CER content in the composites as expected.

Swelling degrees (SD) of s-CER, PVA and s-CER/PVA composites (annealed at 373 K) in methanol, water, and FFAs, respectively are summarized in Table 2. PVA readily absorbs water with a SD of 2.06 in water while barely absorbs methanol with a SD of 0.04 owing to its high selectivity of water over alcohol.<sup>35, 36</sup> S-CER absorbs more water than methanol with a SD of 0.69 and 0.56, respectively. In addition, s-CER easily absorbs FFAs with a SD of 0.74 while PVA barely absorbs FFAs with a SD of 0.02. Based on the obtained SD values, we can expect that during the esterification process catalyzed by the s-CER/PVA composite, the produced water molecules will be readily absorbed in PVA dominated regions by forming hydrogen bonds. However, the reactants (i.e., methanol and FFAs) will be preferably absorbed into the s-CER dominated regions. For composites with decreasing s-CER: PVA mass ratios, they absorbed almost the same amount of methanol, but different amounts of water and FFAs. More specifically, increasing the PVA content in the composite favored absorption of water, but not FFAs.

### 3.2 Effect of composite properties on esterification

The s-CER/PVA composites (mass ratio 3: 2) annealed at 323, 373 and 423 K were used in the esterification and the results are shown in Fig. 4(a). It was found that annealing temperature significantly affected the performance of the composites. With the annealing temperature increased from 323 to 373 K, FFAs conversion increased from 78.4 % to 95.0 %. This may be explained by (1)

**Table 2** Swelling degree of the s-CER, PVA, and s-CER/PVA composite with different s-CER: PVA mass ratios in various solvents.

s-CER: PVA mass ratio	Methanol	Water	FFAs
s-CER	0.56	0.69	0.74
2: 1	0.39	1.46	0.47
3: 2	0.40	1.59	0.36
5: 4	0.39	1.67	0.33
1: 1	0.41	1.73	0.29
PVA	0.04	2.06	0.02

the increase of porosity due to annealing (porosity increased from 41.2 % to 54.3 % with annealing temperature increased from 323 K to 373 K, see effect of porosity on esterification in Fig. S1(f)) and (2) the removal of absorbed water from the composite not only favoring esterification but also increasing the density of  $-\text{SO}_3\text{H}$  groups. However, FFAs conversion decreased significantly to 75.2% when the annealing temperature further increased to 423 K. This is consistent with the FTIR and IEC results that  $-\text{SO}_3\text{H}$  groups in s-CER reacted with  $-\text{OH}$  groups in PVA at 423 K, which resulted in the loss of catalytic active sites. Therefore, the composites annealed at 373 K were used in the experiments thereafter.

From the SD results of s-CER/PVA, we expect s-CER and PVA to play different roles in the esterification process and therefore the s-CER: PVA mass ratio would affect the catalytic activity. To evaluate this effect, the composites with different s-CER: PVA mass ratios (1: 1, 5: 4, 3: 2, and 2: 1) were used to catalyze the esterification process. The results along with that catalyzed by PVA, s-CER, and  $\text{H}_2\text{SO}_4$  are shown in Fig. 4(b). FFAs conversion without catalyst was 4.2 %, which may be because FFAs themselves could act as weak acid catalysts in esterification.<sup>37</sup> When PVA was used, FFAs conversion increased to 12.4 %. Since PVA would not provide catalytic reactive sites for esterification, the increase of the conversion could only be attributed to the absorption of water produced by PVA, which promoted the forward reaction. For the esterification catalyzed by sulfuric acid, the reaction proceeded fairly quickly in the initial 3 h as a result of the homogeneous nature of the reaction mixture. The reaction rate leveled off after 3 h and

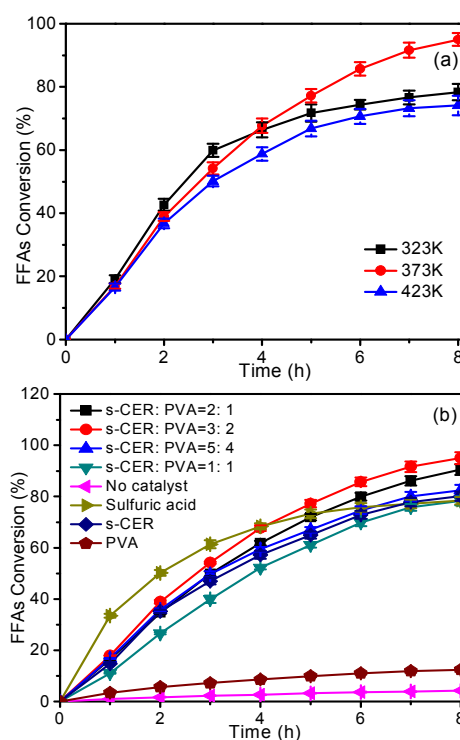
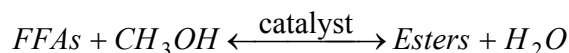


**Fig. 4.** (a) Effect of annealing temperatures on catalytic efficiency of s-CER/PVA (mass ratio 3: 2) for esterification, and (b) Comparison of esterification catalyzed by s-CER, PVA, s-CER/PVA, and  $\text{H}_2\text{SO}_4$  (Reaction conditions: FFAs 20 g, methanol 50 g, catalyst loading 4 g except  $\text{H}_2\text{SO}_4$  (1 g, same number of  $\text{H}^+$  as 4 g s-CER), reaction temperature 338 K and mechanical stirring rate 480 rpm).

the conversion reached 78.4 % in the end (8 h). The esterification catalyzed by ground s-CER was relatively slow at the beginning and the conversion reached 80.1 % after 8 h. FFAs conversion was only 78.3 % by the composite with s-CER: PVA mass ratio of 1: 1, probably because of the lack of catalytic sites in this composite. FFAs conversion increased with the increase of the mass ratio and it reached 95.0 % by the composite with s-CER: PVA mass ratio of 3:2. In addition, the equilibrium FFAs conversion (> 8h) under optimal reaction conditions using s-CER/PVA (mass ratio = 3: 2) reached 97.8 % (Fig. S1(h)). The increase of s-CER content led to the increase of sulfonate groups (indicated by IEC numbers), which led to the increase of catalytic activity. However, the composite with s-CER: PVA mass ratio of 2:1 did not exhibit better catalytic activity, which indicates the important role of PVA in the esterification process.

### 3.3 Esterification kinetics

The esterification of FFAs with methanol can be described as:



During our esterification study, the methanol/FFAs mole ratio was 29: 1 (mass ratio of 2.5: 1), which was high enough to make methanol concentration almost unchangeable at the initial reaction stage. Therefore, the initial reaction kinetics should be able to be treated as a pseudo-first-order if diffusion is not a limiting factor. It is noteworthy that methanol/FFAs mole ratio of 29: 1 is not unusually high as many researches have used higher ratios<sup>38-41</sup> and the excess methanol can be recovered and reused.

We tested the effects of composite thickness (from 0.2 mm to 0.4 mm), composite dimension (from 0.5 cm×0.5 cm to 1.0 cm × 1.0 cm) and stirring rate (from 360 rpm to 600 rpm) on esterification performance and found that all these factors had minimum influence on esterification (shown in Fig. S1(c)-(e)). The effect of composite porosity on esterification was also studied and we found that porosity has little influence when it is larger than 49.5 % (Fig. S1(f)). The porosities of composites annealed at 373K and 423 K are all larger than 50.0 %. Therefore, under our typical reaction conditions, esterification reactions on s-CER/PVA composite are not diffusively controlled but kinetically controlled. Indeed, we tested the esterification at different temperatures using s-CER/PVA annealed at 373 K (Fig. S3) and found the FFAs conversion in the first 4 hours can be very well fitted with a pseudo-first-order reaction kinetics ( $R^2 > 0.99$ ) (Fig. 5(a)). In this way, the reaction rate constant  $k$  at different reaction temperatures can be obtained and the apparent activated energy of the reaction can be calculated using Arrhenius equation (Eq. (1)),

$$\ln k = -E_a / RT + \ln A \quad (1)$$

Where  $k$  is the reaction rate constant ( $\text{h}^{-1}$ ),  $E_a$  is the apparent activation energy ( $\text{kJ mol}^{-1}$ ),  $A$  is pre-exponential factor ( $\text{h}^{-1}$ ),  $R$  is universal gas constant,  $T$  is the reaction temperature (K). As shown in Fig. 5(b), the plot of  $\ln k$  versus  $1/T$  can be represented by a straight line and  $E_a$  is determined to be  $47.8 \text{ kJ mol}^{-1}$ . According to Shi et al. and Singh,<sup>42,43</sup> the esterification reaction is not diffusively controlled but kinetically controlled if the apparent activation energy is high enough (e.g.,  $> 20.0 \text{ kJ mol}^{-1}$ ). The high apparent activation energy of esterification catalyzed by s-CER/PVA composite (i.e.,  $47.8 \text{ kJ mol}^{-1}$ ) further demonstrates that diffusion is not important during our esterification processes. In addition, the apparent activation energies for raw s-CER, ground s-CER and sulfuric acid were also

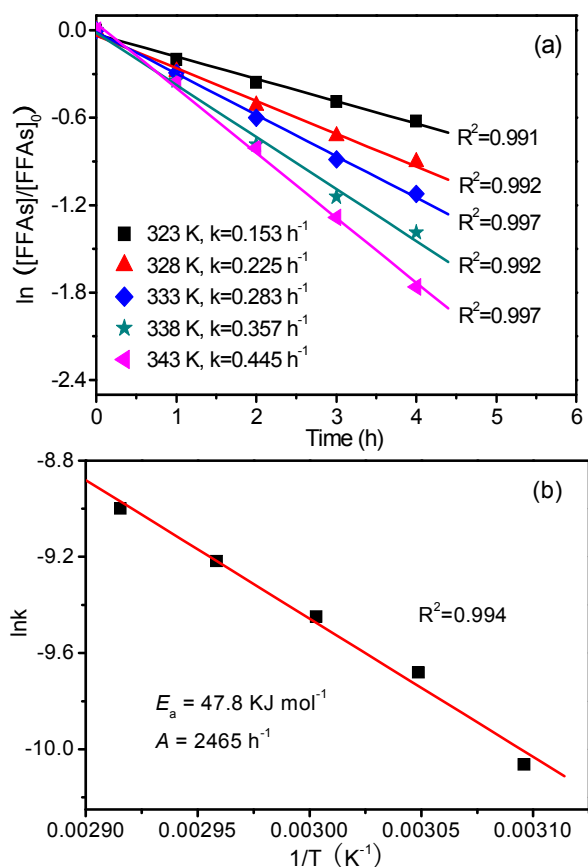


**Fig. 5.** Pseudo-first-order reaction rate constants for esterification catalyzed by s-CER/PVA (mass ratio 3: 2) at different temperatures (a), and the linear Arrhenius equation fitted between  $\ln k$  and  $1/T$  to obtain apparent activation energy  $E_a$  (b). (Reaction conditions: FFAs 20 g, methanol 50 g, catalytic composites loading 4 g and stirring rate 480 rpm).

measured and calculated to be 56.2, 54.7 and  $38.5 \text{ kJ mol}^{-1}$ , respectively. These high apparent activation energies further demonstrate that diffusion is not that important for sulfonate-catalyzed esterification of FFAs with methanol.

### 3.4 Specific role of PVA

The use of TOF values was expected to give a more direct comparison of the catalytic activity in a certain reaction, and a deeper insight into the reaction mechanism.<sup>27</sup> A comparison of the TOF values of different catalysts (calculated from reaction rate constants shown in Fig. S4) is provided in Table 3. The TOF values of s-CER and sulfuric acid were  $1.63 \times 10^{-4}$  and  $2.06 \times 10^{-4} \text{ s}^{-1}$ , respectively, due to the fact that sulfuric acid is homogeneous compared with solid acid s-CER and therefore provide more accessible catalytic sites. Interestingly, the TOF number of the s-CER/PVA composite (s-CER: PVA=3: 2) was approximately 3.3 and 2.6 times greater than that of s-CER and sulfuric acid, respectively, indicating the higher intrinsic catalytic activity of the s-CER/PVA composite.<sup>44,45</sup> As pointed out earlier, the highly hydrophilic -OH sites in PVA can facilitate the absorption of  $\text{H}_2\text{O}$  in the reaction mixture by the PVA dominated region and thus liberate the  $-\text{SO}_3\text{H}$  sites that would otherwise be blocked by  $\text{H}_2\text{O}$  molecules in s-CER or

## Catalysis Science &amp; Technology

## ARTICLE

**Table 3** TOF and produced water of esterification by the s-CER, PVA, s-CER/PVA (with different s-CER: PVA mass ratios), and H<sub>2</sub>SO<sub>4</sub> (Catalytic acid amount (H<sup>+</sup>) of H<sub>2</sub>SO<sub>4</sub> equal to that of s-CER).

Cat.	IEC (mmol g <sup>-1</sup> )	TOF (10 <sup>-4</sup> s <sup>-1</sup> )	FFAs conversion of 8h (%)	Calculated water production (g)	Water in solution (g)	Water in the catalyst (g)
S-CER	5.00	1.63	80.1	0.77	0.15	0.62
2: 1	2.75	3.31	90.5	0.87	0.28	0.59
3: 2	2.01	5.38	95.0	0.91	0.19	0.72
5: 4	1.96	4.40	82.4	0.79	0.02	0.77
1: 1	1.90	3.68	78.3	0.76	0	0.76
PVA	—	—	12.4	0.12	0	0.12
H <sub>2</sub> SO <sub>4</sub>	20.4	2.06	78.2	—	—	—
Blank	—	—	6.8	0.06	—	—

H<sub>2</sub>SO<sub>4</sub> for catalyzing esterification reaction. The higher TOF value for s-CER/PVA than those of s-CER and H<sub>2</sub>SO<sub>4</sub> indicates that a greater number of -SO<sub>3</sub>H were utilized in s-CER/PVA for esterification due to water absorption by PVA. The composites with s-CER: PVA mass ratio of 3: 2 had the highest TOF number among all the s-CER/PVA, suggesting that the PVA content had little effect on the intrinsic catalytic activity after -OH content reached a critical value (PVA mass ratio of 40.0 %). At this point, the -OH groups in PVA were able to maximally attract the water produced away from the -SO<sub>3</sub>H groups. When the s-CER: PVA mass ratio increased to 2:1 (PVA content reduced), the TOF value of the composite decreased, indicating that the PVA amount is not sufficiently large to attract the water produced at this mass ratio. The relationship between the PVA mass content and the TOF value is plotted in Fig. S5.

The water contents in the solution after esterification reaction were analyzed and the results are also listed in Table 3. The measured water contents were much lower than the calculated value based on the conversion rate. Clearly, water produced was indeed absorbed in the catalytic composite and primarily in the PVA region. It is well known that esterification of FFAs with methanol is a reversible reaction. Since the water produced was absorbed into the PVA region in the composite, the reaction would be driven to the right. This is clearly demonstrated by the higher FFAs conversion with s-CER/PVA composites compared with s-CER and H<sub>2</sub>SO<sub>4</sub>. Therefore, PVA must have played a dual role in the esterification reaction, liberating the -SO<sub>3</sub>H sites for esterification and pushing the reaction forward. To further ensure that water was absorbed in the composites, SD of the composites after reaction in water was measured (Table S5). The value decreased greatly if the composite was only air dried but the values remained almost constant if the composites were vacuum dried at 373 K. Therefore, water produced was truly absorbed by the composite, which decreased its SD in water. We further note that the constant and direct contact of PVA with s-CER in the s-CER/PVA composite provides more driving forces for the diffusion of produced H<sub>2</sub>O out of s-CER to PVA than the case of simple mixing of s-CER and PVA, which resulted in higher FFAs conversion (Fig. S6).

A striking observation in our study is the higher TOF value of heterogeneous -SO<sub>3</sub>H in s-CER/PVA than that of homogeneous -SO<sub>3</sub>H in H<sub>2</sub>SO<sub>4</sub>. Due to the heterogeneous nature, sulfonated solid acids should have lower TOF values than sulfuric acid, which was commonly observed in many past studies.<sup>46,47</sup> The 2.6 times higher TOF of s-CER/PVA than sulfuric acid suggests that the water less, heterogeneous sulfonate sites are more reactive than water-blocked homogeneous ones.

To further verify the point that PVA enhances the esterification efficiency through removing produced water and to evaluate how much water PVA can take to facilitate esterification, water was deliberately added into the system before the reaction (Fig. S7). For ground s-CER, the FFAs conversion decreased from 80.1 % to 32.0 % when adding 1 g of water, due to the poisoning of catalytic sites by water. However, for s-CER/PVA, the FFAs conversion only decreased from 97.5 % to 82.8 % by adding same amount of water but decreased sharply after adding over 2 g of water (< 50.0 %), which suggests PVA can at least absorb certain amount of water to mitigate its side effect before the catalyst needs to be dried.

### 3.5 Esterification process catalyzed by s-CER/PVA composite

The esterification process by s-CER/PVA is proposed based on the well-known mechanism of esterification catalyzed by s-CER<sup>16,48</sup> and is illustrated in Fig. 6. Catalytic esterification occurs following the steps of: 1) protonation at the carbonyl oxygen of FFAs via the acidic composite and generation of carbocation; 2) positive nucleophilic attack at the positive carbon atoms by the hydroxyl group in methanol and the generation of an unstable intermediate; 3) removal of the proton from the unstable intermediate and production of fatty acid methyl ester (FAME) and water; 4) diffusion of FAME and water out of resin pores to surface; 5) absorption of water by the hydroxyl groups of PVA through forming hydrogen bonds; and 6) transfer of FAME and non-absorbed water from the interface region to the liquid phase.

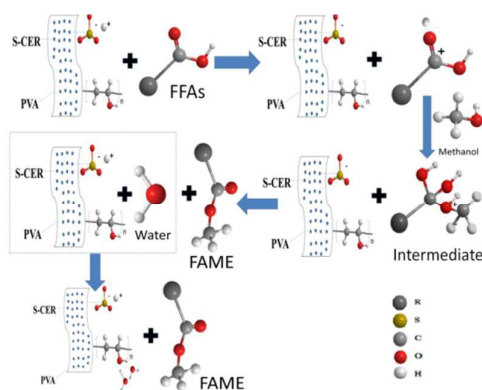


**Fig. 6.** Proposed esterification process catalyzed by s-CER/PVA composite.

Our GC results showed that all four major FFAs have been almost completely converted to their corresponding esters and the final product distribution is methyl laurate 16.6 %, methyl myristate 4.2 %, methyl hexadecanoate 22.0 % and methyl linoleate 54.0 % (Fig. 7). In addition, the conversion of the four FFAs and the yield of esters matched well at designated time points (mass balance almost 100 %), which are also consistent with the titration results (Fig. S8). The yield of the four esters was almost same (~97.0 %) although our results from separate batch tests using single acid suggest that the esterification of dodecanoic acid may have preference over other three acids and oleic acid (Table S6). Nonetheless, the high conversion of all tested single acids with s-CER/PVA (> 93.0 %) under primary reaction conditions suggest s-CER/PVA is an efficient esterification catalyst.

### 3.6 Reusability of the catalytic composites

Besides the catalytic activity, reusability of catalyst is very important in saving production cost. The ground s-CER and s-CER/PVA (s-CER: PVA=3: 2) composite were employed in esterification under optimal reaction conditions for six runs and the results are compared in Fig. 8. The optimal reaction conditions were determined to be: methanol/FFAs mass ratio 2.5: 1 (equivalent to molar ratio 29: 1), catalyst/solution mass ratio 1: 14, catalyst loading 5 g, reaction temperature 338 K and mechanical stirring rate 480 rpm (see Fig. S1 for details).

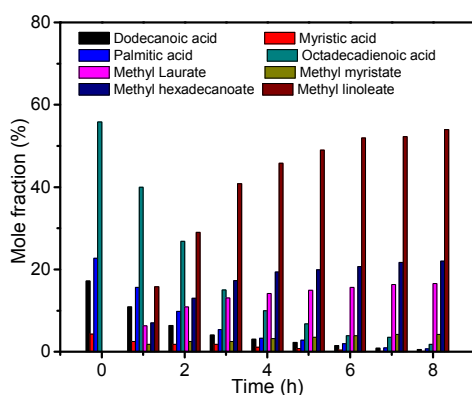


**Fig. 7.** The evolution of the four component FFAs and their corresponding FAME during the esterification process catalyzed by s-CER/PVA (mass ratio 3:2) under optimal reaction conditions.

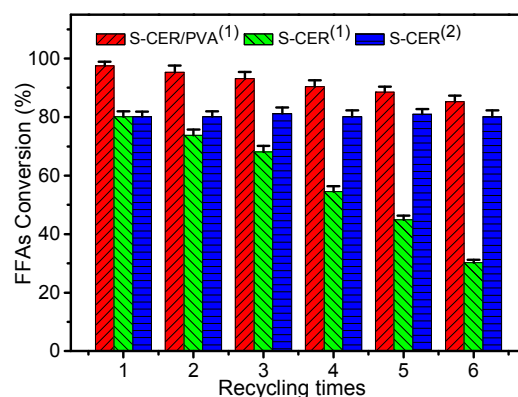


**Fig. 8.** The catalytic performances of ground s-CER and s-CER/PVA versus recycling times under optimal reaction conditions (<sup>1</sup>The catalyst was not treated before reuse; <sup>2</sup>The catalyst was washed and vacuum dried at 373 K for 24 h before reuse).

The ground s-CER exhibited much lower catalytic activity than s-CER/PVA and its catalytic activity decreased sharply in the following runs. The FFAs conversion reduced from 80.1 % in the 1st run to 30.2 % in the 6th run if the s-CER was not treated after reaction. However, if the s-CER was washed and vacuum dried at 373 K for 24 h to remove the absorbed water, its catalytic activity did not change even after the 6th run. This clearly suggests that the absorption of water produced from esterification to s-CER is the main reason accounting for the decrease of its catalytic activity.

S-CER/PVA showed excellent catalytic activity for esterification of FFAs (97.5 % conversion) and the catalytic activity decreased only mildly after six runs (FFAs conversion reduced to 85.0 %). The IEC of s-CER/PVA after six runs was only slightly decreased but its SD in water was significantly reduced if the composites were not treated. However, if the composite was washed and dried at 373 K, its SD in water can be fully recovered, suggesting the water produced was absorbed in s-CER/PVA (see Table S5 for details). Therefore, PVA enhances the reusability of s-CER/PVA by absorbing the water produced and maintaining the reactive -SO<sub>3</sub>H sites.

It has been pointed out that the leaching of -SO<sub>3</sub>H groups is a common problem for sulfonated catalysts.<sup>37, 47, 49</sup> Therefore, the leaching of sulfur from s-CER/PVA was investigated by analyzing the elemental composition of s-CER/PVA before and after reaction and we found no leaching of S from the catalyst even after 6 runs (Table S7), which is consistent with the IEC results (unchanged after 6 runs, Table S5). This information also demonstrated that the loss of catalyst reactivity was not due to the leaching of s-CER from PVA matrix, but due to the absorption of water produced, which is mitigated in the s-CER/PVA composite. Also, the sulfur contents in the reaction mixture before and after each esterification run tested by micro-coulometric analyzer were almost the same (~140 ppm, Table S8), which further confirms that there was no leaching of sulfur from s-CER/PVA composite during esterification reaction.

## 4. Conclusions

We have developed an s-CER/PVA composite as a heterogeneous catalyst for efficient esterification of FFAs separated from WCO. In the catalyst, s-CER is responsible for providing reactive sulfonate sites while PVA for absorbing and removing water produced, and liberating reactive sites for catalysis. Higher FFAs conversion and



## ARTICLE

## Journal Name

TOF values can be obtained using the s-CER/PVA catalytic composite compared with s-CER or sulfuric acid alone. The catalytic composite is reusable, with a slight decrease after 6 cycles of utilization, because the water produced was largely absorbed by PVA. The use of PVA in the catalytic composites may offer new ideas to design solid acid catalysts that remove products with side effects (i.e., water) in esterification and any other solid acid catalyzed reactions with water production.

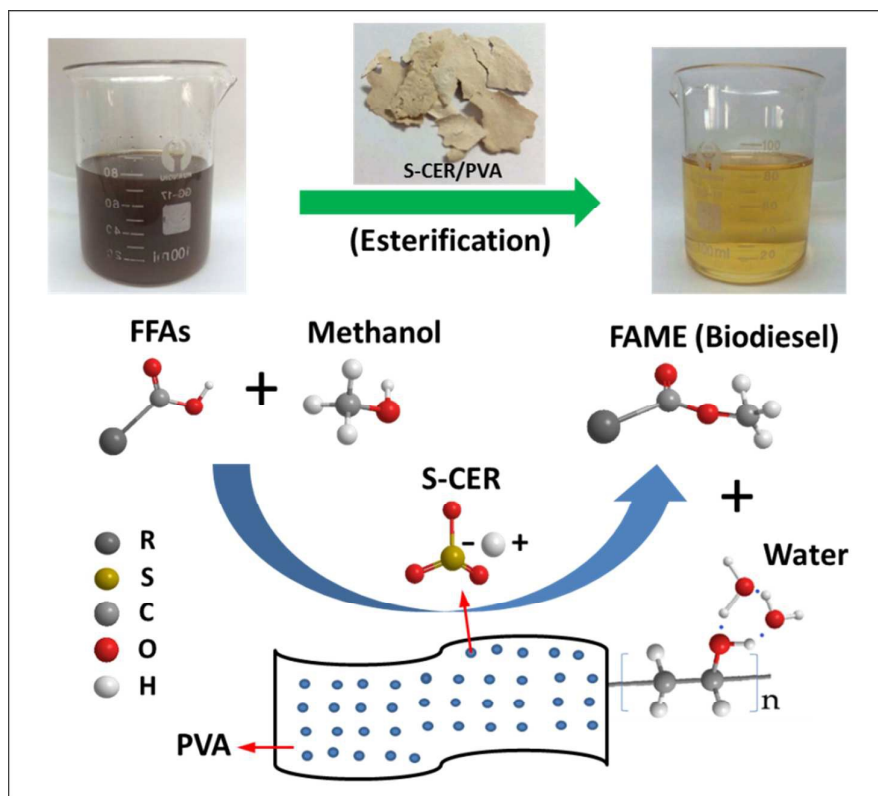
### Acknowledgements

This research was partially supported by the National Natural Science Foundation of China (No. 51308312), Ningbo Bureau of Science and Technology under its Innovation Team Scheme (2012B82011) and Major Research Scheme (2012B10042), and the Ningbo Municipal Government (3315 Plan and the IAMET Special Fund, 2014A35001-1).

### Notes and references

1. M. Toda, A. Takagaki, M. Okamura, J. N. Kondo, S. Hayashi, K. Domen and M. Hara, *Nature*, 2005, **438**, 10.
2. R. Luque, J. C. Lovett, B. Datta, J. Clancy, J. M. Campelo and A. A. Romero, *Energy Environ Sci*, 2010, **3**, 1706.
3. H. Li, D. Gao, P. Gao, F. Wang, N. Zhao, F. Xiao, W. Wei and Y. Sun, *Catal Sci Tech*, 2013, **3**, 2801.
4. R. Luque, L. Herrero-Davila, J. M. Campelo, J. H. Clark, J. M. Hidalgo, D. Luna, J. M. Marinas and A. A. Romero, *Energy Environ Sci*, 2008, **1**, 542.
5. K. Suwannakarn, E. Lotero, K. Ngaosuwan and J. James G. Goodwin, *Ind Eng Chem Res*, 2009, **48**, 2810.
6. A. Birla, B. Singh, S. N. Upadhyay and Y. C. Sharma, *Bioresour Technol*, 2012, **106**, 95.
7. K. Malins, V. Kampars, J. Brinks, I. Neibolte and R. Murnieks, *Appl Catal, B*, 2015, **176-177**, 553.
8. J. M. Marchetti and A. F. Errazu, *Biomass Bioenergy*, 2008, **32**, 892.
9. K. Fukuhara, K. Nakajima, M. Kitano, H. Kato, S. Hayashi and M. Hara, *ChemSusChem* 2011, **4**, 778.
10. S. Suganuma, K. Nakajima, M. Kitano, S. Hayashi and M. Hara, *ChemSusChem* 2012, **5**, 1841.
11. K. Wilson and A. F. Lee, *Catal Sci Tech*, 2012, **2**, 884.
12. N. Özbay, N. Oktar and N. A. Tapan, *Fuel*, 2008, **87**, 1789.
13. H. Zhang, J. Ding, Y. Qiu and Z. Zhao, *Bioresour Technol*, 2012, **112**, 28.
14. H. Zhang, J. Ding and Z. Zhao, *Bioresour Technol*, 2012, **123**, 72.
15. R. Wang, H. Li, F. Chang, J. Luo, M. A. Hanna, D. Tan, D. Hu, Y. Zhang, B. Song and S. Yang, *Catal Sci Tech*, 2013, **3**, 2244.
16. R. Tesser, L. Casale, D. Verde, M. Di Serio and E. Santacesaria, *Chem Eng J*, 2010, **157**, 539.
17. R. Tesser, M. D. Serio, L. Casale, G. Carotenuto and E. Santacesaria, *Can J Chem Eng*, 2010, **88**, 1044.
18. F. Lode, S. Freitas, M. Mazzotti and M. Morbidelli, *Ind Eng Chem Res*, 2004, **43**, 2658.
19. M. Zhu, B. He, W. Shi, Y. Feng, J. Ding, J. Li and F. Zeng, *Fuel*, 2010, **89**, 2299.
20. J. Hao, M. Gong, Y. Wu, C. Wu, J. Luo and T. Xu, *J Hazard Mater*, 2013, **244-245**, 348.
21. M. M. Ibrahim, A. Koschella, G. Kadry and T. Heinze, *Carbohydr Polym*, 2013, **95**, 414.
22. S. Das, A. K. Banthia and B. Adhikari, *Indian J Chem Technol*, 2007, **14**, 552.
23. D. S. Pito, I. M. Fonseca, A. M. Ramos, J. Vital and J. E. Castanheiro, *Bioresour Technol*, 2009, **100**, 4546.
24. L. Guerreiro, P. M. Pereira, I. M. Fonseca, R. M. Martin-Aranda, A. M. Ramos, J. M. L. Dias, R. Oliveira and J. Vital, *Catal Today*, 2010, **156**, 191.
25. C. S. Caetano, L. Guerreiro, I. M. Fonseca, A. M. Ramos, J. Vital and J. E. Castanheiro, *Appl Catal, A*, 2009, **359**, 41.
26. J. Ding, B. He and J. Li, *J Biobased Mater Bioenergy*, 2011, **5**, 1.
27. G. Moretti, *Catal Lett*, 1994, **28**, 143.
28. D. Kim, *J Membr Sci*, 2004, **240**, 37.
29. D. Kim, H. Park, J. Rhim and Y. Lee, *Solid State Ionics*, 2005, **176**, 117.
30. W. Shi, B. He, J. Ding, J. Li, F. Yan and X. Liang, *Bioresour Technol*, 2010, **101**, 1501.
31. J. A. Macia-Agull, M. Sevilla, Maria A. Diez and A. B. Fuertes, *ChemSusChem*, 2010, **3**, 1352.
32. G. Socrates, *Infrared and Raman Characteristic Group Frequencies, 3rd ed.*, Wiley, New York, 2005.
33. K. Koyama, M. Okada and M. Nishimura, *J Appl Polym Sci*, 1982, **27**, 2783.
34. J. H. Chen, Q. L. Liu, A. M. Zhu and Q. G. Zhang, *J Membr Sci*, 2008, **320**, 416.
35. W. Chiang and C. Chen, *Polymer*, 1998, **39**, 2227.
36. J. Rhim, H. Park, C. Lee, J. Jun, D. Kim and Y. Lee, *J Membr Sci*, 2004, **238**, 143.
37. X. Mo, D. E. López, K. Suwannakarn, Y. Liu, E. Lotero, J. James G. Goodwin and C. Lu, *J Catal*, 2008, **254**, 332.
38. C. Poonjarernsilp, N. Sano and H. Tamon, *Appl Catal, B*, 2014, **147**, 726.
39. C. Pirez, J.-M. Caderon, J.-P. Dacquin, A. F. Lee and K. Wilson, *ACS Catal*, 2012, **2**, 1607.
40. C. Pirez, A. F. Lee, J. C. Manayil, C. M. A. Parlett and K. Wilson, *Green Chem*, 2014, **16**, 4506.
41. J. Dhainaut, J.-P. Dacquin, A. F. Lee and K. Wilson, *Green Chem*, 2010, **12**, 296.
42. W. Shi, B. He and J. Li, *Bioresour Technol*, 2011, **102**, 5389.
43. A. Singh and S. Fernando, *Chem Eng Technol*, 2007, **30**, 1716.
44. A. Takagaki, C. Tagusagawa and K. Domen, *Chem Commun*, 2008, **42**, 5363.
45. C. Tagusagawa, A. Takagaki, A. Iguchi, K. Takanabe, J. N. Kondo, K. Ebitani, T. Tatsumi and K. Domen, *Chem Mater*, 2010, **22**, 3072.
46. L. Geng, G. Yu, Y. Wang and Y. Zhu, *Appl Catal, A*, 2012, **427-428**, 137.
47. Y. Liu, E. Lotero and J. James G. Goodwin, *J Catal*, 2006, **242**, 278.
48. J. Li, Y. J. Fu, X. J. Qu, W. Wang, M. Luo, C. J. Zhao and Y. G. Zu, *Bioresour Technol*, 2012, **108**, 112.
49. D. E. López, J. James G. Goodwin and D. A. Bruce, *J Catal*, 2007, **245**, 381.

## Graphical abstract:



PVA enhances the catalytic activity and reusability of s-CER/PVA for esterification by absorbing the water produced and liberating the reactive  $-\text{SO}_3\text{H}$  sites.